An Asteroid and its Moon Observed with LGS at the SOR[1]

Jack Drummond, Odell Reynolds, and Miles Buckman

Air Force Research Laboratory, Directed Energy Directorate, RDSS
3550 Aberdeen Ave SE, Kirtland AFB, NM 87117-5776

ABSTRACT

The faint moon, Romulus, around the main belt asteroid (87) Sylvia was detected and followed over 6 nights in March and May of 2015, using adaptive optics and a laser guide star on the 3.5 m telescope at the Starfire Optical Range. Romulus was $\sim$ 81 times fainter than V=12.5 Sylvia at 1.2 μm. From these observations we are able to derive an orbit for the satellite, calculate Sylvia's mass, and derive its density of 1.37±0.04 gm/cm^3. These observations closely mimic a small man-made geosynchronous satellite approaching a larger one, and make our 3.5 m telescope the smallest ground-based telescope to ever image any asteroids moon.

1. Introduction

For the past few years the Starfire Optical Range (SOR) has been testing the limits of our Adaptive Optics (AO) system to detect Closely Spaced Objects (CSO) with our 3.5 m telescope in support of SDA (Space Domain Awareness). We have used the Washington Double Star (WDS) catalog to identify close companions with high brightness ratios, but inevitably found that high Δ mags were less than reported. Most catalogue Δ mags are derived at visual wavelengths ($\lambda = 0.55\mu$m), while we typically observe at longer wavelengths, either 0.8 or 1.2μm. In coeval (formed at the same time) binaries the fainter companion is redder, and therefore at longer wavelengths appears brighter with respect to the primary component, lowering the Δ mag, and reducing their usefulness for our detection of CSO testing.

Therefore, we recently began a program to detect the satellites of asteroids, a dozen or so of which have been imaged by 8-10 m telescopes. These objects are better choices for us in our CSO project since they both shine by reflected sunlight and are presumably of the same composition and albedo which means that should have the same Δ mag at all wavelengths. Furthermore, the orbital periods of these (generally) small moons are on the order of days, and, depending on the Earth-asteroid geometry, the orbit of the moon around its parent asteroid can be relatively open, allowing us to follow it around the asteroid, or closed, merging in and out of the asteroid PSF. Most asteroids are in the 10-15 magnitude range of geosynchronous satellites (GEOs), and most

[1]AMOS Technical Conference 2015

moons are 5 magnitudes or more fainter than the asteroid. Altogether, these characteristics make asteroid moons ideal test objects for us, closely mimicking small man-made satellites approaching larger ones – the CSO problem.

It took a while for us to develop the right strategy to find these moons, as we report below, but on 2015 March 23, we finally detected the small moon Romulus around the Main Belt asteroid (89) Sylvia. Romulus was discovered with the Keck 10 m telescope in 2001 (Brown et al 2001) and has been followed ever since on 8 and 10 m telescopes. It has been the subject of two recent studies, by Fang et al (2012) and Berthier et al (2014), so that this system also provides some space truth for us. We detected the moon on 6 nights (and failed to detect it on several others) between March 23 and April 29, making the 3.5 m telescope the smallest ground-based telescope to ever image any asteroid's moon. From measuring Romulus' position with respect to Sylvia we have derived its orbit and the mass of the system. Then by combining this mass with previous determinations of Sylvia's volume, we have also derived Sylvia's density, a notoriously difficult quantity to determine short of a spacecraft flyby.

The point of this current paper is to report the successful detection schemes and to recount the methods for measuring separations and Δ mags. For more information, see the paper to be submitted to *Icarus* this year (Drummond et al 2015; in preparation).

2. Observations and Measurements

On 2015 March 23, with our 3.5 m telescope using LGS AO, we targeted V=12.5 asteroid (89) Sylvia. Suspected visually by the test director (the second author), it was confirmed the next morning with post-imaging processing, and subsequently observed several more times. Altogether, some 68 images of Romulus were measured on 6 nights between 2015 March 23 and May 29, and 3 more were found in our archives from 2012 November 12. Observations consisted of sets of 10, 20, 40 and 60 sec integrations, usually saturating the asteroid by 40 sec. Interestingly, if the moon could be seen at any integration time, it could be seen in all, albeit less clearly at shorter integration times.

For all of these observations, a sodium laser with 40 W out of the top of the launch telescope produced a laser guide star (LGS) for higher order AO correction, while the light from the asteroid itself provided tip-tilt correction. The system uses a 24x24 Shack-Hartmann wave front sensor (WFS), and in this case, I-band light (0.9μm) is diverted to the track-focus sensor, while imaging in the J-band (1.2μm).

2.1. Detections

The most promising method for faint CSO detections is to subtract the PSF of the unresolved asteroid and search for the faint signal of the companion in the residuals. As has been previously determined, the AO PSF is Lorentzian in shape (Drummond 1998; Drummond et al 2014). Therefore, we fit the mean of each integration set of observations as a single Lorenztian and subtract the model. The residuals from subtracting a Lorentzian from the image should scatter about a mean of zero; this is the basis of least squares. However, this never seemed to expose any candidates among the many artifacts that appear in the images due to camera and other defects. Late in the game we discovered that rather than subtracting the model from the data, if we divide the data by the model and take the log, which should scatter about unity, a faint signal is detected more easily among the artifacts. Figure 1 illustrates all of this for our first detection of Romulus. All further detections of Romulus put the moon on one side or the other, indicating that Earth was close to the orbital plane of the moon.

2.2. Measurements

After the asteroid's moon is detected there still remains the problem of measuring the moon's position and brightness with respect to the asteroid. We have used several methods, ordered here by our preference:

1. Simultaneously fit both components as either independent Lorentzians or Lorentzians having the same shape – the isoplanatic assumption.
2. Fit each component separately, cutting out a subsection centered on the moon even if the much brighter asteroid intrudes. See Fig 2.
3. Fit the asteroid as a Lorentzian, subtract the model, and then fit a subsection of the residuals for the moon. See Fig 2.
4. Click on the peak of the asteroid and the moon and record their positions and peak pixel values.

In the case of Sylvia and Romulus, not one of the images allowed us to make a simultaneous fit (method 1), but then neither did we have to resort to method 4. Of the 71 images measured, 40 were measured with method 2 and 31 with method 3.

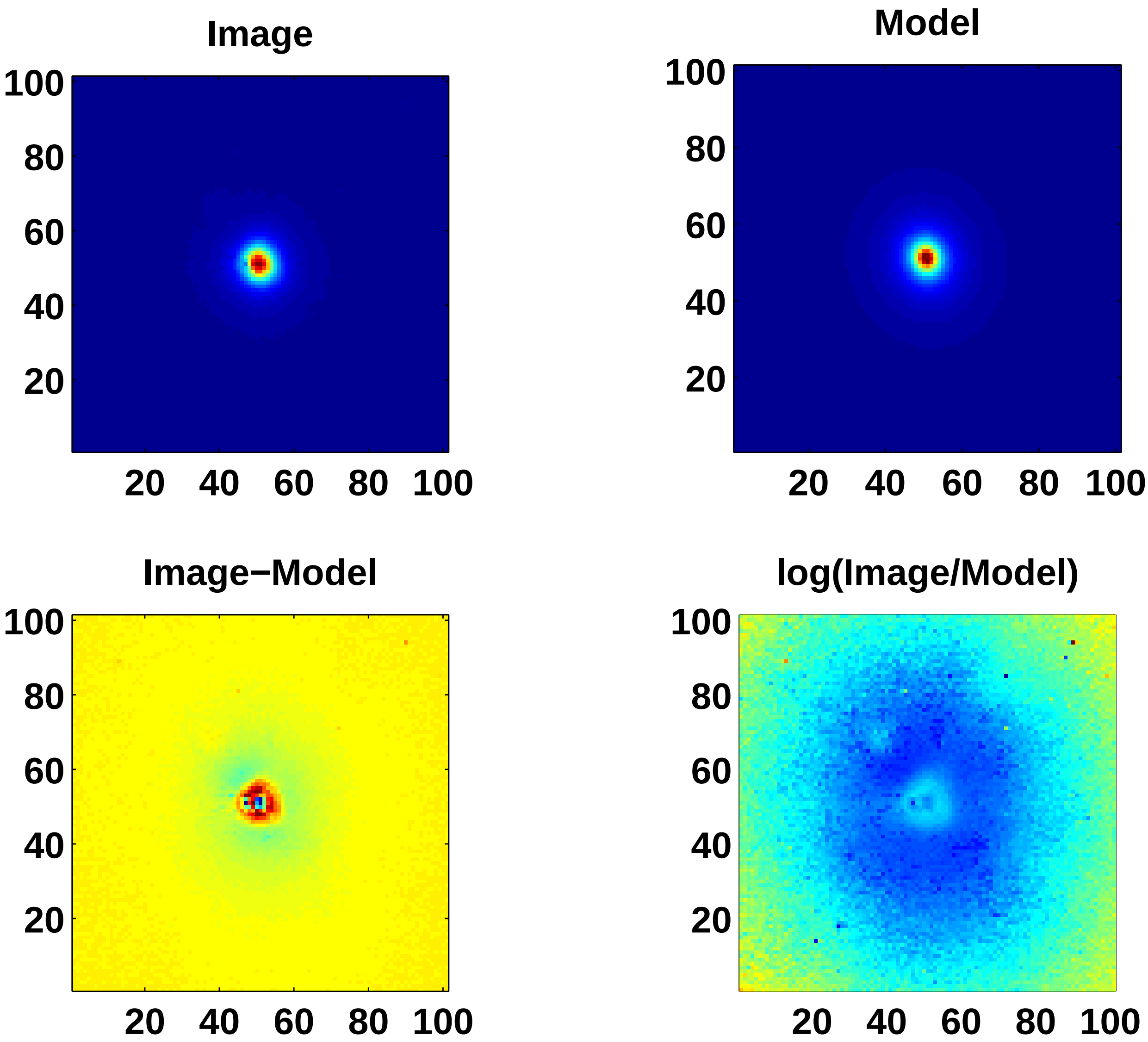

Fig. 1.— The fit of our first detection of Romulus. At upper left is the mean of five 10 sec observations, at upper right is the Lorentzian fit to the asteroid, and at lower left is the difference between the image and the model. The moon is very difficult to see in the residuals and can easily be overlooked. At bottom right, the moon shows up much better in the log of the ratio of the image and model. The axes are pixels.

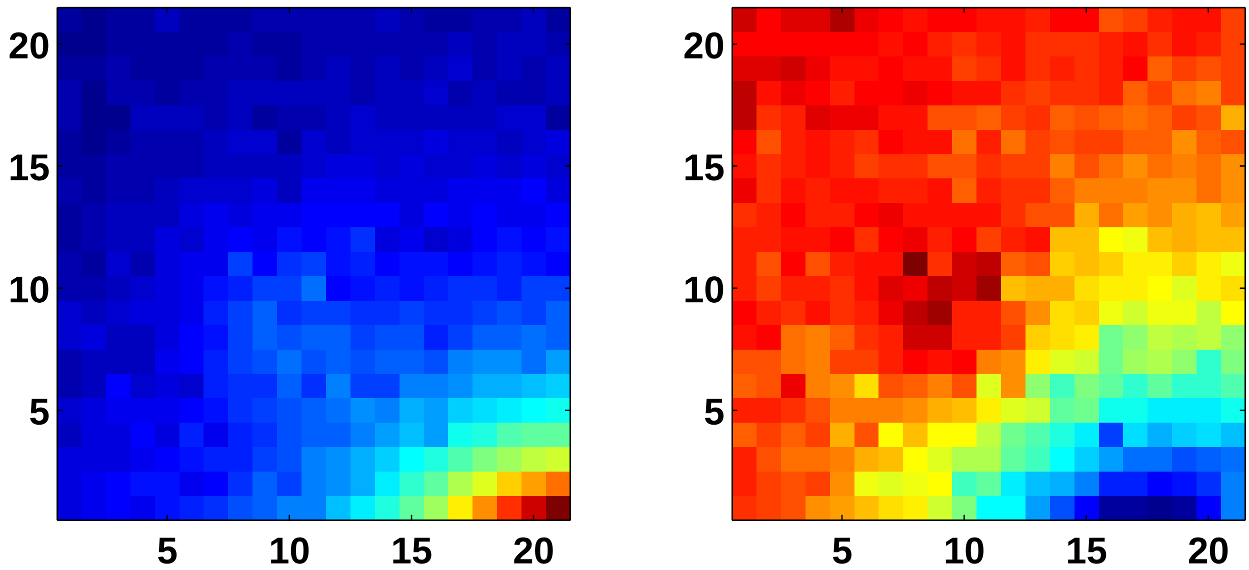

Fig. 2.— Methods 2 and 3 for measuring Sylvia and Romulus. At left, a small subsection of the image can be fit for Romulus. Or, at right, a subsection of the lower left subplot in Figure 1, residuals from the fit of Sylvia can be fit for Romulus. Notice the intrusion of Sylvia from the lower right. In this case only method 3 could be performed, i.e., converged to a solution. The axes are pixels.

3. Conclusions

Figure 3 shows the positions of Romulus, where the 71 measured positions are condensed down to 11 distinct times, superimposed on the orbit we derive from our images. We only detected Romulus at elongations, out to 0.67″ (3.2 μm), and never less than 0.4″ (1.9 μm) away from Sylvia. Figure 4 shows the elliptical apparent orbit and the true circular orbit plotted over the USA, as well as the actual size and shape of Sylvia derived by inverting lightcurves (Durech et al 2011). With the orbital semimajor axis of 1355 km and the 3.6412 day period, together with the volume from Durech et al (2011), we derive a bulk density of 1.37 ± 0.04 gm/cm^3, in agreement with Fang et al (2012) and Berthier et al (2014).

The difficulty of detecting and measuring the moon around an asteroid is quite similar to detecting and measuring the approach of a small satellite to a larger one at GEO. The average Δ mag between Romulus and Sylvia was 4.8 in the J-band, a factor of ~ 81 in area or ~ 9 in diameter, which by extension to GEOs, would be two objects of 36 and 4 m in diameter. Observations of asteroids with moons will continue to be useful targets for the SOR to hone our CSO capability.

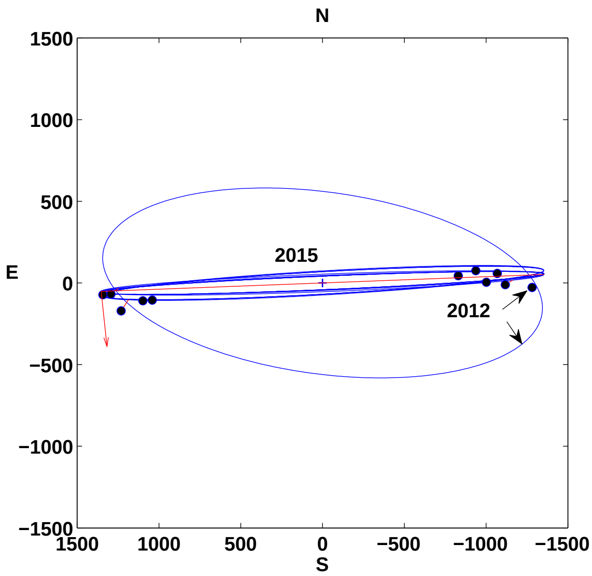

Fig. 3.— Orbit of Romulus with SOR data. Individual apparent orbits and lines of nodes (red lines across ellipse in 2015) are drawn for each data point, where the orbit for the one point from 2012 stands out as the more open ellipse. The axes are km at the asteroid.

Fig. 4.— Orbit of Romulus and size and shape of Sylvia to scale, over the USA. While the apparent orbit of Romulus was highly elliptical to us in 2015, the true orbit is circular.

Acknowledgments

We gratefully thank the many night crews for their dedication and hard work on long and sometimes apparently pointless nights.

References

Berthier J., F. Vachier, F. Marchis, J.Durech, B. Carry, 2014, Icarus 239, 118.

Brown, M.E., J.L. Margot, W.M Keck II, I. de Pater, H. Roe, 2001. Central Bureau Electronic Telegrams 7588.

Drummond, J. 1998, Proc. SPIE, 3353, 1050.

Drummond, J.D., B. Carry, W.J. Merline, C. Dumas, H. Hammel, S. Erard, A. Conrad, P. Tamblyn, C. R. Chapman, 2014, Icarus 236, 28.

Durech, J., M. Kaasalainen, D. Herald, D. Dunham, B. Timerson, J. Hanus, E. Frappa, J. Talbot, T. Hayamizu, B.D. Warner, F. Pilcher, A Galad, 2011, Icarus 214, 652.

Fang, J., J.L. Margot, P. Rojo, 2012, Astrophys. J. 144, 70.